The Influence of Wing Flexibility on the Elevator Angle to Trim for a Sailplane in Steady Glide

Jan Kacprzyk, Miron Nowak
Technical University of Warsaw
Chair of Mechanics

Presented at the XIth OSTIV Congress at Leszno, Poland

Introduction

One of the important static stability characteristics of a sailplane is the elevator angle required to trim η_T and its dependence on speed U. A typical example of this function is shown in Fig. 1. As we know in the case of neutral static stability of the sailplane, the same elevator setting is required to trim for all flight velocities.

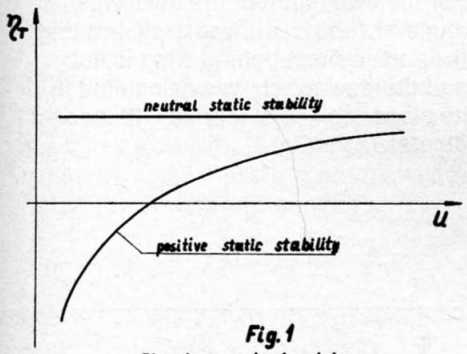

Fig. 1
Elevator angle to trim

From flight tests made for many contemporary sailplanes the shape the elevator angle to trim versus velocity curve usually differs greatly from the theoretical one obtained [1] for a rigid sailplane. This indicates that a more exact analysis of this problem which takes into account the effects of aeroelasticity is required.

The elevator angle to trim depends on the incidence of the tailplane and force required to trim the sailplane. The change of drag forces due to elastic deflections of the sailplane is small and its influence on the pitching moment of the aerodynamic forces about the centre of gravity of the structure (c. g.) can be neglected. Then the change (L_T^e) due to elastic deformations, of the lift (L_T) at the tail will depend only on the aerodynamic span load distribution due to wing distortions. This influence exists only for swept wings. For wings whose line of aerodynamic centers is perpendicular to the flight direction the moment of the aerodynamic forces of the wing about the c. g. of the sailplane depend only on the total lift but not on the lift distribution along the span.

The angle of attack of the tail α_T is determined by the incidence of the wing α_o the downwash angle at the tail ε and the tailplane setting i_T relative to the zero lift line of the wing (Fig. 2).

$$\alpha_T = \alpha_o + i_T - \varepsilon \tag{1}$$

In the case of an all-moving tailplane, i_T denotes the setting of the zero lift line of the tailplane. For an elastic sailplane each of the terms appearing in eq. (1) is a sum of two components, one corresponding to the rigid structure (denoted below by the subscript "r") and the second to the increment due to elastic distortion (denoted below by the subscript "e"). In this case the angle α_o should be taken as the angle of attack of the cross section of the wing in the plane of symmetry, and along the span we have

$$\alpha(y) = \alpha^r(y) + \alpha^e(y) \quad \text{and} \tag{2}$$
$$\alpha^e(y) = \alpha_o^e + \Theta(y) \tag{2a}$$

where α_o^e defines the change of this angle in the cross section $y = 0$ (that is the change of fuselage inclination relative to the flight path) and $\Theta(y)$ denotes the elastic twist of the wing. The change i_T^e is due to tailplane torsion and fuselage bending produced by the lift on the tail. The downwash angle $\varepsilon(y) = \varepsilon^r(y) + \varepsilon^e(y)$ describes the aerodynamic interference between wing and tail and $\varepsilon^e(y)$ due to the change of lift distribution on the wing corresponding to $\alpha^e(y)$. In the present analysis, the effect of fuselage bending and tailplane torsion will be neglected and only the case of a straight wing (without sweep) when the total lift on the wing ($L_W = L_W^r + L_W^e$) and on the tail ($L_T = L_T^r + L_T^e$) do not change by the elastic distortion of the sailplane will be considered. The sailplane velocity and (small) angle of flight path will be assumed as being constant. Thus the following conditions must be satisfied:

$$L_W^e = 0 \qquad L_T^e = 0 \tag{3}$$

The first of these expressions is used to calculate α_o^e and the second will be used to determine the change of the

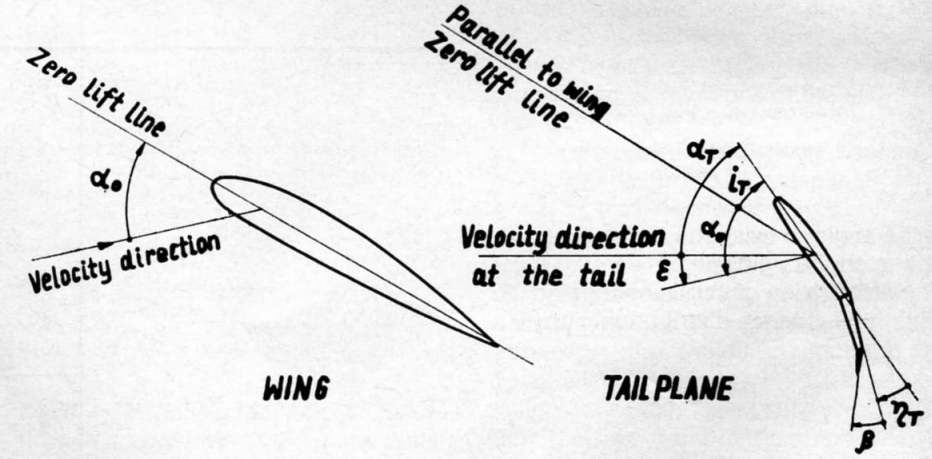

Fig. 2
Wing - tailplane configuration

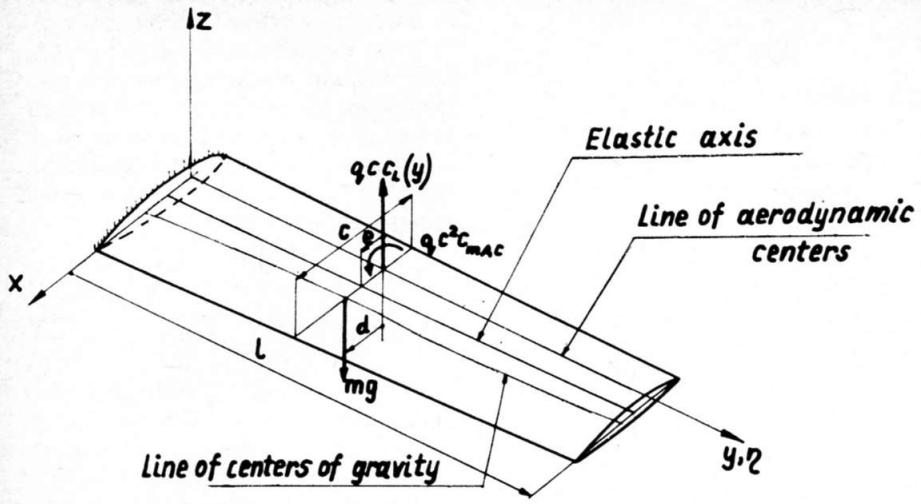

Fig. 3
Wing loads

elevator angle to trim due to wing distortion.

Torsional wing deflection

From (3) it is possible to obtain the lift distribution on the wing and the incidence angle α_o^e using the elastic equilibrium equation for the wing only. This method is well known and precisely discussed for example in [2] but for convenience the most important steps will be briefly recalled.

Denoting the dynamic pressure by q, wing section lift coefficient by $c_l(y)$ and wing torsion flexibility influence function by $C^{\Theta\Theta}(y,\eta)$ using the notation given in Fig. 3 we obtain the following equation

$$(4)\qquad \Theta(y) = q\int_o^l C^{\Theta\Theta}(y,\eta)\, e(\eta)\, cc_l^e(\eta)\, d\eta + f(\eta)$$

where

$$(5)\qquad f(y) = q\int_o^l C^{\Theta\Theta}(y,\eta)\,[c_{m_{AC}} c^2(\eta) + e(\eta) cc_l^e(\eta)]\, d\eta + g\int_c^l C^{\Theta\Theta}(y,\eta)\,[d(\eta) - e(\eta)]\, m(\eta)\, d\eta$$

is the angle of twist due to the loads acting on the rigid wing.

The distribution of cc_l^e is connected with the incidence distribution α^e by the relation

$$(6)\qquad \alpha^e(y) = \mathcal{A}(cc_l^e)$$

where $\mathcal{A}$ denotes the aerodynamic operator of the wing whose form depends on the assumed aerodynamic theory. For sailplane wings with high aspect-ratio, Prandtls lifting line theory gives sufficient accuracy and in this case

$$(7)\qquad \mathcal{A}(cc_l) = \frac{cc_l(y)}{cc_{l\alpha}(y)} + \frac{1}{8\pi}\int_{-l}^{+l} \frac{d(cc_l)}{d\eta}\,\frac{d\eta}{y-\eta}$$

Using in the numerical calculations sets of numerical values of functions given in the form of column matrices

$$\{cc_l^e\} \text{ and } \{\alpha^e\}$$

the itegro-differential operator $\mathcal{A}$ can be replaced by one square matrix [A] of aerodynamic influence coefficients. In the illustrative example of calculations presented below, the matrix [A] has been obtained by the collocation (Glauert) method, using the series

$$(8)\qquad cc_l(y) = \sqrt{l^2 - y^2}\sum_{r=0} a_r\, U_r\left(\frac{y}{l}\right)$$

where a_r ($r = 0, 2, 4, \ldots$) are constant coefficients and U_r are the Tchebysheff polynomials of the second kind and of order r. Because of the symmetry of the wing loading only coefficients with even subscripts appear in the series (8) however the number of terms of this sum is equal to the number of elements of the column matrix.

Using the Gauss-Multhopp quadrature formula for the evaluation of the definite integral in (4) we obtain from (3) and (4) a system of algebraic equations for the determination $\{cc_l^e\}$ and α_o^e

$$(9)\qquad \begin{bmatrix} [A] - q[E]\{-1\} \\ \lfloor 1 \rfloor \quad [W] \qquad 0 \end{bmatrix} \begin{bmatrix} \{cc_l^e\} \\ \alpha_o^e \end{bmatrix} = \begin{bmatrix} \{f\} \\ 0 \end{bmatrix}$$

where $[E] = [C^{\Theta\Theta}][e][W]$ and $[W]$ is the diagonal weighting matrix for Multhopp's quadrature.

The downwash at the tail

For the evaluation of the downwash angle ε^e (and ε^r) it was assumed that the vortex sheet behind wing is flat and the downwash was calculated in its plane ($z = 0$) at a point with coordinates (x,y) (Fig. 4).

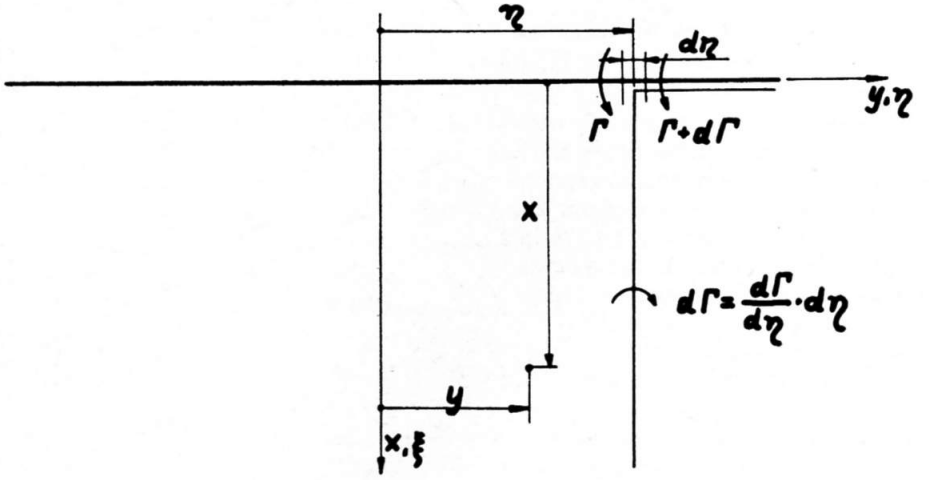

Fig. 4
Vortex sheet behind wing

The velocity induced by the bound velocity with intensity $\Gamma(\eta)$ is

$$w_1(x,y) = -\frac{1}{4\pi}\int_{-l}^{+l} \frac{\Gamma(\eta)\,d\eta}{[x^2+(y-\eta)^2]^{\frac{3}{2}}}$$

and the velocity induced by the free vorticity is

$$w_2(x,y) = -\frac{1}{4\pi}\int_{-l}^{+l}\frac{d\Gamma}{d\eta}(y-\eta)\int_0^{\infty}\frac{d\xi}{[(x-\xi)^2+(y-\eta)^2]^{\frac{3}{2}}}$$

After addition of both terms and simple transformation we obtain

$$(10)\qquad w(x,y) = -\frac{1}{2\pi}\int_{-l}^{+l}\frac{d\Gamma}{d\eta}\frac{d\eta}{y-\eta} - \frac{1}{4\pi}\int_{-l}^{+l} L(y,\eta)\frac{d\Gamma}{d\eta}d\eta$$

where

$$(10a)\qquad L(y,\eta) = \frac{\sqrt{1+\left(\frac{y-\eta}{x}\right)^2}-1}{y-\eta} \qquad (\lim_{\eta\to y} L(y,\eta) = 0)$$

The circulation $\Gamma(\eta)$ is connected with $cc^1(\eta)$ by the relation

$$(11)\qquad \Gamma(\eta) = \frac{U}{2}\,cc_l(\eta)$$

The downwash angle at the tail can be calculated using in (10) for x the distance x_T between aerodynamic centers of wing and tailplane

$$(12)\qquad \varepsilon(y) = -\frac{w(x_T,y)}{U}$$

After substitution of the series (8) in (10) we can evaluate the first integral analytically, and the second one by using the n point Gauss-Mehler's quadrature [3]. Wherefrom we obtain

$$(13)\qquad \varepsilon(y) = \sum_{r=0}(r+1)\left[U_r\left(\frac{y}{l}\right) - \frac{1}{2\pi}\sum_{i=1}^{n} L(y,\eta_i)\,T_r(\eta_i)\right]a_r$$

where T_r is the Tchebysheff polynomial of the first kind and of order r. Knowing the matrix $\{cc_l\}$ we can obtain the coefficients a_r from (8). In this way we obtain finally the matrix $[A_{WT}]$ of aerodynamic wing-tail influence coefficients. Using it we can compute the downwash angle as follows

$$(14)\qquad \{\varepsilon\} = [A_{WT}]\{cc_l\}$$

The values of cc_l^e in the admissible flight velocity range are usually smaller than cc_l^r, however ε^e can be greater than ε^r because the downwash is determined by the derivative $\frac{d(cc_l)}{d\eta}$.

The elevator angle to trim

The increment of elevator angle due to wing flexibility can be calculated from the condition (3):

$$(3a)\qquad \frac{1}{2}L_T^e = q\int_0^{l_T} c_T c_{l_T}^e(y)\,dy = 0$$

where l_T denotes the semi-span of the tailplane and $c_T c_{l_T}^e$ the product of tailplane chord and tail lift coefficient connected with the angles α_T^e, η_T^e and β^e by the tailplane aerodynamic operator $\mathcal{A}_T$ similarly to the wing operator $\mathcal{A}$ (7)

$$(15)\qquad \bar{\alpha}_T^e = \mathcal{A}_T(c_T c_{l_T}^e)$$

where $\bar{\alpha}_T^e$ is an equivalent angle of attack which takes into account the elevator angle.

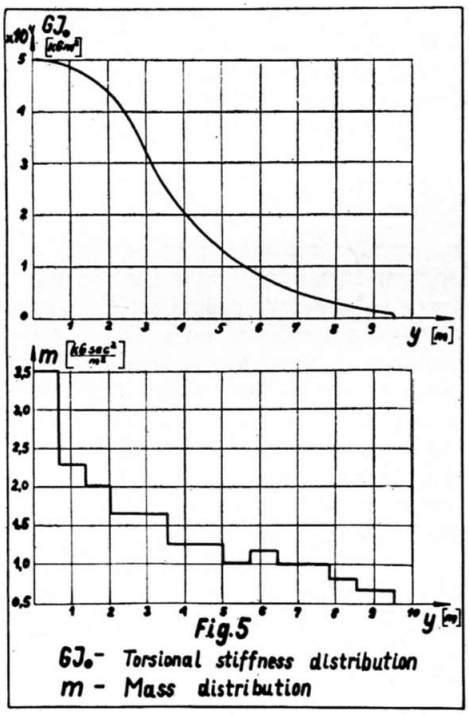

Fig.5

GJ_0 - Torsional stiffness distribution
m - Mass distribution

When the elevator is fitted with a geared tab and the gear ratio is k:

$$\beta = k\eta_T$$

then

$$(16)\qquad \bar{\alpha}_T^e = \alpha_T^e + \frac{c_{l\eta_T} + k\,c_{l\beta_T}}{c_{l\alpha_T}}\eta_T^e = \alpha_T^e + \bar{a}\,\eta_T^e$$

where

$$c_{l\eta_T} = \frac{\partial c_{l_T}}{\partial \eta_T},\quad c_{l\alpha_T} = \frac{\partial c_{l_T}}{\partial \alpha_T} \text{ and } c_{l\beta_T} = \frac{\partial c_{l_T}}{\partial \beta}$$

are the derivatives for two-dimensional flow. The coefficient $c_{l\beta_T}$ is not equal to zero only along the tab span. We evaluate the integrol (3a) by Multhopp's quadrature with the weighting matrix $[W_T]$ and substituting (15), (16) and (1) we obtain

$$\{\bar{\alpha}\} = \alpha_0^e\{1\} - [A_{WT}]\{cc_l^e\} + \eta_T^e\{\bar{a}\} = [A_T]\{c_T c_{l_T}^e\}$$

and

$$[1]^T[W_T][A_T]^{-1}(\alpha_0^e\{1\} - [A_{WT}]\{cc_l^e\} + \eta_T^e\{\bar{a}\}) = 0$$

which yield the following expression for the elastic contribution to the elevator angle to trim

$$(17)\qquad \eta_T^e = \frac{[1]^T[W_T][A_T]^{-1}(\alpha_0^e\{1\} - [A_{WT}]\{cc_l^e\})}{[1]^T[W_T][A_T]^{-1}\{\bar{a}\}}$$

The corresponding equation for the rigid wing can be written as follows

$$[1]^T[W_T][A_T]^{-1}(\alpha_0^r\{1\} + i_T\{1\} - [A_{WT}]\{cc_l^r\} + \eta_T^r\{\bar{a}\}) = L_T$$

thus

$$(18)\qquad \eta_T^r = \frac{L_T - [1]^T[W_T][A_T]^{-1}(\alpha_0^r\{1\} + i_T\{1\} - [A_{WT}]\{cc_l^r\})}{[1]^T[W_T][A_T]^{-1}\{\bar{a}\}}$$

To take into account the effect of fuselage deflection we must add an additional term $i_T^e\{1\}$ in the parenthesis of (17).

Example of calculations

The method of analysis indicated above has been applied to a contemporary high-performance sailplane which has a maximum speed of 300 km/h and the following essential data:

Wing span — 19.0 m. Wing area 15.7 m². Aspect ratio 23. Tailplane span 3.6 m. Distance between the aerodynamic center axes of wing and tailplane 4.32 m. The sailplane has an all-moving tailplane with geared tab. The tab span is 1.88 m and the gear ratio k = 2.1. The torsional rigidy and mass distribution along the semi-span of the wing are given in Fig. 5. Results obtained correspond to flight at altitude of 1 km and 3 values of all-up weight W = 405, 440, and 460 kg and corresponding c. g. locations of the sailplane.

The typical variation with flight speed of the change of fuselage inclination angle α_0^e and downwash angle at the tail ε^e due to elastic distortion of the wing is shown in Fig. 6. For comparison the downwash angle for a rigid sailplane is also given on Fig. 6. The angle α_0^e shows the direct effect of wing twist and although in the speed range considered its absolute value is small, the lift distribution on the elastic wing differs greatly from the lift distribution on the rigid wing. The effect of this change of lift distribution is the change in aerodynamic interference between wing and tail expressed

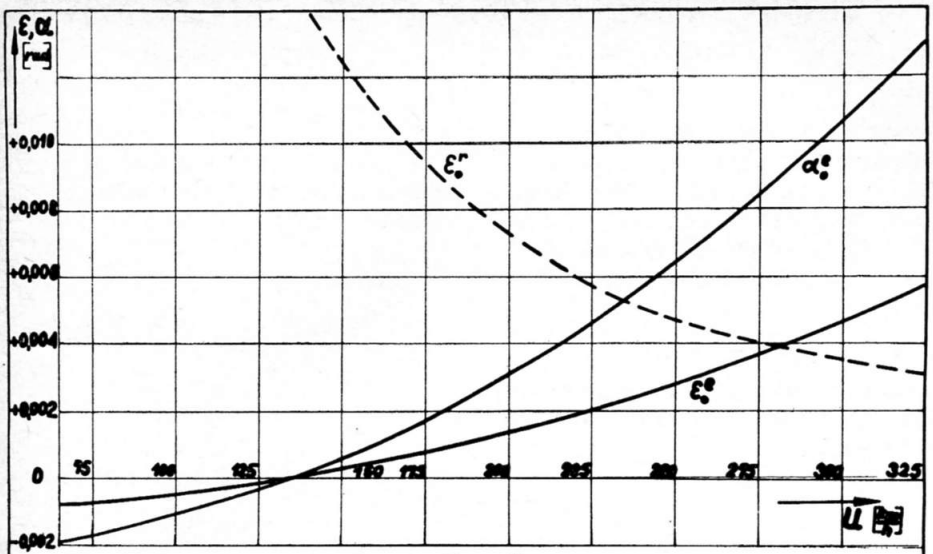

Fig. 6
Change of the fuselage angle of inclination and downwash angle at the tail due to deflections on the wing

by the downwash at the tail. Only the downwash angle in the plane of symmetry of the sailplane is given on Fig. 6 but the calculations show that the variation of this angle along the tailplane span is small.

For high speeds, the change of downwash due to wing torsion is greater than the downwash of the rigid wing. This results from the fact, that the shape of the lift curve for the rigid wing is smoother than for the elastic wing. Neglecting the variation of downwash angle along the tailplane span and the effect of the tab, the distance between the ordinates α_o^e and ε^e expresses roughly the increment of the elevator angle to trim due to elasticity. As can be seen from the diagram, for the example treated in the whole speed range, the change of downwash angle is approximatively proportional to the change of inclination of the fuselage. Because the absolute value of α_o^e is greater than the absolute value of ε^e and its influence on the change of the elevator angle to trim, as results from (1), is opposite, hence the direct influence of the wing twist is predominant and the downwash due to wing torsion reduces this effect.

As the aim of analysis given is the investigation of the influence of wing flexibility only, the influence of fuselage flexibility is not considered here. However it should be mentioned that for high speeds, the tailplane lift is negative and is of the order of sixty and more kilograms. This produces an increment of tail setting relative to wing. Therefore this increases the unfavorable aeroelastic effects at the tailplane because the angle α_o^e and i_T appear in eq. (1) with the same sign.

The variation with speed of the elevator angle to trim for the example treated and three all up weights is shown in Fig. 7. For comparison the curves obtained assuming a rigid structure are also given. It is seen from the diagrams that for high speeds the slope of the curves becomes negative and this can cause trimming difficulty because the elevator angle to trim has to be reduced for an increase in speed. It should be mentioned that the divergence speed of this sailplane is about 660 km/h, which is much higher than the speed range considered, where already the effects of aeroelasticity are important.

The results obtained for one chosen example have been discussed and it cannot be deduced that this applies to all other sailplanes. It can be said, however, that for contemporary high-performance sailplanes with high design speeds, the effects of aeroelasticity must be taken into account not only by considering the dynamic effects (for example the flutter analysis) but also by considering the static stability and manoeuvrability.

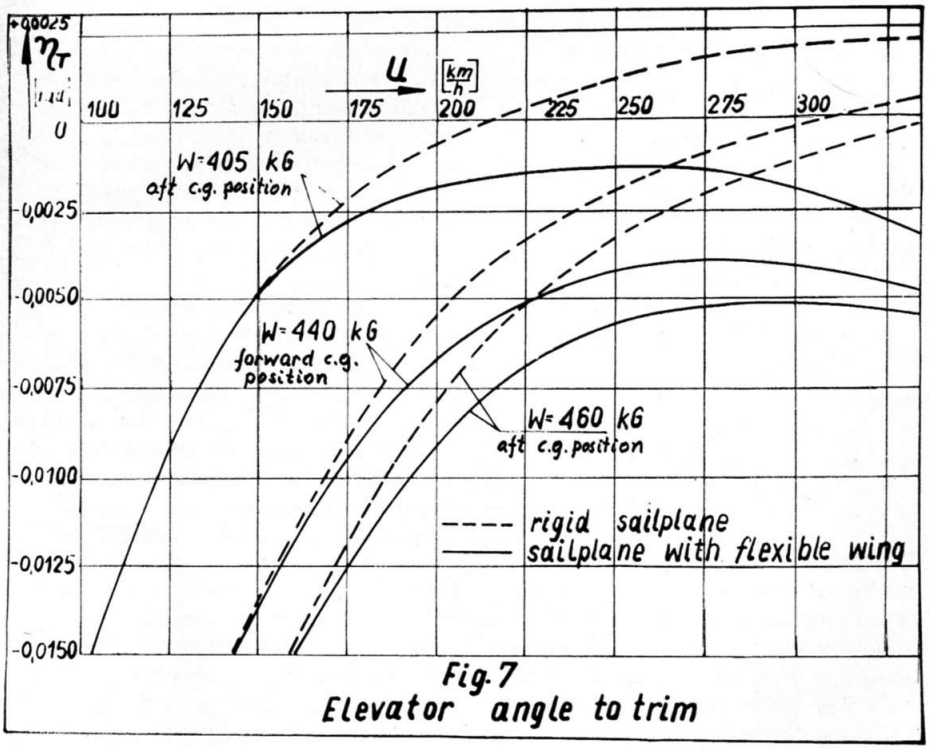

Fig. 7
Elevator angle to trim

References

1. Etkin, B.; Dynamics of flight, John Wiley & Sons, Inc., New York 1958.
2. Bisplinghoff, R. L., Ashley H., Halfman R. L.: Aeroelasticity, Addison-Wesley Publ. Comp., Cambridge 42, Mass., 1955.
3. Kopal Z.: Numerical Analysis, Chapman & Hall Ltd., London, 1961.